Identifying and characterizing regulators of histone acylation and replication stress

Kollenstart, L.

CHAPTER 5

Replication-IDentifier: a genome-wide approach to identify regulators of replication fork progression and stability

Leonie Kollenstart*, Amandine Batte*,
Sophie van der Horst and Haico van Attikum

* Equal contribution

ABSTRACT

Faithful replication of DNA during S-phase is essential for cell survival and genomic stability. This is challenged by DNA damage from both endogenous and exogenous sources that can block replication fork progression. To ensure faithful DNA replication, cells have evolved elaborate signaling pathways to stabilize and repair stalled replication forks. However, our understanding of the repertoire of and interplay between factors in replication fork maintenance is rather limited. To systematically identify factors that stabilize and repair stalled replication forks, we developed a genome-wide approach, named Replication-IDentifer (Repli-ID), to directly interrogate replication fork stability and progression by tracking the replicative DNA polymerase ε (Pol ε) in thousands of yeast mutants in parallel. Using Repli-ID under replication stress conditions, we uncovered 85 genes that affect Pol ε levels at replication forks, including several genes that have previously not been connected to replication fork maintenance. Follow-up studies revealed that the identified *NSR1* and *ROX1* genes affect Pol ε progression. Moreover, we show that loss of Rox1 leads to replication fork instability and increased replication stress. Thus, Repli-ID has provided a unique resource for the identification and further characterization of factors involved in replication fork progression and stability.

INTRODUCTION

Faithful DNA replication during S-phase is essential for cell survival and genome stability. However, during replication, cells can encounter many types of exogenous and endogenous DNA damage, resulting in replication fork stalling. For example, DNA adducts and interstrand crosslinks (ICLs) can impede replication fork progression. Drugs like hydroxyurea (HU), on the other hand, deplete the dNTP pool, causing replication forks to stall. The incorrect restart of stalled replication forks can lead to a collapse of these structures and result in the formation of DNA double-strand breaks (DSBs). Ultimately, this can lead to genome instability and the onset of cancer (Gaillard et al., 2015). To prevent this, cells deal with replication fork stalling and instability by invoking a replication stress response that promotes cell cycle arrest, the stabilization of stalled forks, and transcription of ribonucleotide reductase (RNR) genes, while suppressing late origin firing (Branzei and Foiani, 2009; Pardo et al., 2017; Zeman and Cimprich, 2014).

HU-induced replication stress results in the formation of single-stranded DNA (ssDNA) stretches which become coated by the RPA complex (Rfa1-Rfa2-Rfa3) (Alani et al., 1992). The emergence of ssDNA is the trigger for the recruitment and activation of the kinase Mec1 (hATR) and its co-factor Ddc2 (hATRIP), leading to initiation of the intra-S-phase checkpoint response (Rouse and Jackson, 2002; Zou and Elledge, 2003). The full activation of Mec1 requires additional factors such as the PCNA-like clamp complex 9-1-1 and Dbp11 (hTopBP1). After the 9-1-1 complex is loaded onto DNA near ssDNA-dsDNA junctions, its subunit Ddc1 activates Mec1 (Majka and Burgers, 2003). In turn, Ddc1 phosphorylation by Mec1 allows for the recruitment of Dbp11, which strongly stimulates Mec1 kinase activity (Mordes et al., 2008; Paciotti et al., 1998; Puddu et al., 2008). Once Mec1 is fully activated, it phosphorylates the Rad53 kinase, thereby transducing and amplifying the the intra-S-phase checkpoint response. In addition, several replisome components have been implicated in promoting Rad53 activation, including the Sgs1 helicase (homologue of WRN helicase) and Mrc1 (hClaspin) (Alcasabas et al., 2001; Bjergbaek et al., 2005; Cejka et al., 2010; Cobb et al., 2003; Hegnauer et al., 2012; Katou et al., 2003; Osborn and Elledge, 2003; Tanaka and Russell, 2001). Besides promoting Rad53 activation, Mrc1 also acts in conjunction with other replisome components, such as Tof1 and Csm3, to stabilize paused replication forks during HU-induced replication stress (Bando et al., 2009; Katou et al., 2003).

When cells face a limiting amount of dNTPs, replication is further halted by the repression of late origin firing. This is dependent on the Rad53-mediated phosphorylation of initiation factors Sld3 and Dbf4 (Lopez-Mosqueda et al., 2010; Zegerman and Diffley, 2010). To promote replication restart, Rad53 regulates expansion of the dNTP pool by inducing the expression of RNR genes (Chabes et al., 2003; Morafraile et al., 2015). In addition to the RNR genes, the

expression of various other DNA damage response genes is induced by Rad53, for instance by inhibiting the Nrm1 transcriptional repressor (Travesa et al., 2012). Collectively, this illustrates the complex molecular network required for full checkpoint activation by Mec1 and Rad53, which is critical to stabilize replication forks in order to continue DNA synthesis after fork arrest (Cobb et al., 2003; Katou et al., 2003; Sogo et al., 2002; Tercero and Diffley, 2001).

This highly complex system of preventing and resolving replication stress requires many levels of regulation which are not yet fully understood. To discern how cells deal with replication stress, it is crucial to identify all factors involved in this response. For this reason, many high-throughput functional genomics and phenotypic screens were employed to identify genes implicated in preventing and resolving replication stress (Chang et al., 2002; Hartman and Tippery, 2004; Parsons et al., 2006; Woolstencroft et al., 2006). Most of these methods are based on indirectly measuring replication stress responses through cell survival. However, methods to directly measure replication fork stability, particularly in a genome-wide manner, were lacking. To bridge this gap, we developed a novel technique, termed Replication-IDentifer (Repli-ID). This systematic approach measures the enrichment of a replisome component, in unperturbed or replication stress conditions, by chromatin immunoprecipitation (ChIP) on two unique DNA barcodes during DNA replication in yeast deletion mutants. Consequently, Repli-ID quantitively measures replication fork integrity and progression in thousands of yeast mutants in parallel. Using Repli-ID, we identified 85 genes affecting the accumulation of the replicative polymerase Pol ε near an origin of replication under conditions of HU-induced replication stress. Among these were many genes involved in transcription regulation and chromatin organization. Functional assays revealed how two genes, *NSR1* and *ROX1*, play a role in S-phase entry and replication fork stability, respectively. Thus, Repli-ID provides a robust and innovative strategy to directly investigate replisome stability and progression in unperturbed and replication stress conditions in a high-throughput manner. Since no strategies exist to profile replication forks in high-throughput, we expect the Repli-ID strategy can be highly valuable for interrogating replication fork dynamics at defined genomic loci.

RESULTS

Repli-ID: a new method to identify regulators of replication fork stability in yeast

To identify genes that affect replication fork stability, we developed a novel tool that directly interrogates replication fork stability in thousands of yeast mutants in parallel. This method employs a systematic approach that finds its basis in the ChIP-based barcode screening methods Epi-ID and Epi-Decoder (Korthout et al., 2018; Vlaming et al., 2016). Epi-ID quantitively

measures post-translation modifications on DNA barcodes inserted at the *HO* locus. These barcodes function as molecular identifiers for single deletion mutants, enabling the interrogation of chromatin status in large pools of yeast mutants in parallel (Vlaming et al., 2016). In Epi-Decoder, the DNA barcodes were introduced in the TAP-tagged yeast library, allowing for the identification of TAP-tagged proteins that bind the barcoded *HO* locus (Korthout et al., 2018). Based on Epi-ID and Epi-Decoder, we aimed at developing Repli-ID to study replication fork stability in yeast deletion mutants by studying the binding of replisome components near a barcoded origin of replication. To this end, yeast mutants will be employed in which two unique DNA barcodes, flanking a KanMX selection marker, are located near the origin of replication ARS404 (Figure 1A). The ARS_BC barcode is located at ARS404, while the ARS+1.6_BC barcode is located 1.6kb away from ARS404 (Figure 1A). Following ChIP of Pol2-9xMyc, which is the catalytic subunit of the leading strand DNA polymerase ε and to which we will further refer as Pol ε (Cobb et al., 2003; Masumoto et al., 2000), on the pool of mutant cells, the amount of Pol ε in a single yeast mutant is represented by the abundance of the corresponding barcode across all barcodes. This abundance, which will be determined by Next-Generation Sequencing (Figure 1B-C), serves as a measure for replisome progression/stability at the barcode.

Towards establishing Repli-ID

To establish Repli-ID, we first investigated recruitment of Pol e-9xMyc to ARS404, as well as the early firing origin ARS607, which served as a control (Figure S1A) (Cobb et al., 2003; Masumoto et al., 2000). Wild-type cells were synchronized in G1 by α-factor treatment. Next, α-factor was washed out and cells were released into S-phase in medium containing 0.2M HU (Figure S1A). Recruitment of Pol ε at ARS607 was observed at 40 minutes after release and was detected at 4kb away from the origin at 60 minutes (Figure S1B), agreeing with earlier reports (Cobb et al., 2003; Masumoto et al., 2000). In contrast, recruitment of Pol ε to ARS404 was not observed, suggesting a lack of firing of ARS404 (Figure S1B) as was shown in another study (Tsai et al., 2015). Thus, ARS404 may behave as is a late firing or dormant origin.

During replication stress, late origin firing is repressed by Rad53-dependent phosphorylation of Sld3 and Dbf4 (Lopez-Mosqueda et al., 2010; Zegerman and Diffley, 2010). While in the absence of Rad53, origin firing is no longer suppressed (Lopez-Mosqueda et al., 2010; Zegerman and Diffley, 2010), Rad53-deficient cells fail to resolve various forms of replication stress, leading to the collapse of stalled replication forks (Kim and Weinert, 1997; Sogo et al., 2002; Tercero and Diffley, 2001). To circumvent these adverse effects, we employed a strain expressing mutant forms of Sld3 and Dbf4 (*sld3-38A dbf4-4A*) that cannot be phosphorylated by Rad53. Overexpression of Sld3-38A and Dbf4-4A can bypass the Rad53-mediated repression of origin firing. However, under these conditions, checkpoint activation and cell viability remain unaffected and replication fork progression continues

after arrest (Zegerman and Diffley, 2010). This strain was generated by integrating a galactose-inducible *sld3-38A dbf4-4A* construct at the *BAR1* locus in a strain expressing Myc-tagged Pol ε. In the *Pol ε-9xmyc sld3-38A dbf4-4A* strain, Sld3-38A and Dbf4-4A overexpression was induced by adding galactose 30 minutes prior to release in S-phase in 0.2M HU- and glucose-containing medium. Under these conditions, both ARS607 and ARS404 showed efficient recruitment of Pol ε after release into S-phase (Figure S1C), with a moderate delay in progression to ARS607+4kb compared to wild-type (Figure S1B). Since the *Pol ε-9xmyc sld3-38A dbf4-4A* strain allows early firing of ARS404, we continued setting up the Repli-ID system using this strain.

To create the yeast strains for the Repli-ID screen, we crossed the *Pol ε-9xmyc sld3-38A dbf4-4A* strain with the barcoder mutant library using SGA technology (Figure 1A). The resulting Repli-ID library contained around ~4500 barcoded mutants and ~1100 barcoded wild-types as a control. To study the effect of pooled gene deletions on Pol ε stability, we performed Pol e-9xMyc ChIP-qPCR on a selected pool of ~1100 barcoded mutants, using a wild-type pool of ~1000 barcoded strains as a control. Both pools showed equal recruitment of Pol ε to ARS404 (Figure S1D), suggesting no apparent effect of individual mutants in the pool on the overall recruitment of Pol ε to the barcodes. Moreover, at 40 minutes after release in S-phase, recruitment of Pol ε

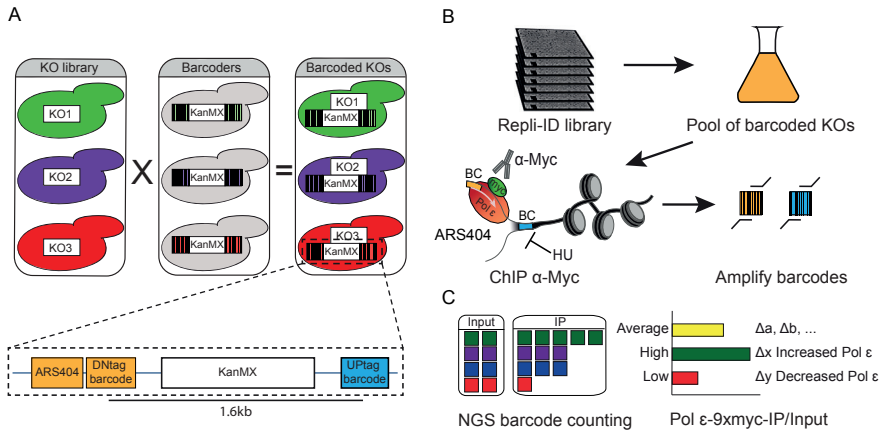

Figure 1. Repli-ID: a new concept to identify regulators of replication fork stability.
(A) Construction of the Repli-ID library. Knock-out and DaMP libraries of yeast mutants were crossed to a Barcoder library of yeast strains containing Pol e-9xMyc using SGA technology. Each strain in the Barcoder library contains a KanMX selection gene flanked by unique 20bp UpTag and 20bp DownTag barcodes integrated at the HO locus (B) Outline of Repli-ID. Strains from the Repli-ID library were pooled and grown in in liquid medium. Pools of cells were arrested in G1 and subsequently released in G1 in the presence of 0.2M HU. Next, they were subjected to ChIP of Pol e-9xMyc using anti-Myc antibody. The barcodes were amplified from ChIP and input DNA. (C) Next-generation sequencing of barcodes. Barcodes were counted in immunoprecipitates (IP) and input. Abundance of Pol ε was measured by adjusting barcode levels in ChIP to those in the input.

peaked at ARS_BC (Figure S1D). For ARS+1.6_BC, Pol ε reached maximal occupancy around 60 to 80 minutes (Figure S1D). Therefore, we assigned 40 and 80 minutes into S-phase as time points for sample collection during the actual Repli-ID screens.

Repli-ID screens identify new regulators of replication fork stability

For the Repli-ID screens, the collection of barcoded yeast mutants was pooled and synchronized in G1 with α-factor during which galactose was added to induce overexpression of Dbf4-4A and Sld3-38A. After washing away the α-factor, cells were released into S-phase in 0.2M HU- and glucose-containing medium. Samples were collected at 40 and 80 minutes in S-phase and subjected to ChIP of Myc-tagged Pol ε. Barcodes from input and immunoprecipitated DNA samples were amplified by PCR and subsequently identified and counted using Next-Generation Sequencing (Figure 1B). The amount of Pol ε present in a single yeast mutant is reflected by the abundance of a barcode in the immunoprecipitate compared to that in the input (ChIP/input) (Figure 1C). All barcode enrichment data can be found in Table S1. Consistent with our previous results (Figure S1C and S1D), we did not detect a clear accumulation of Pol ε at ARS+1.6_BC at the 40-minute time point and therefore decided to exclude this timepoint/locus from further analysis. However, for ARS_BC at the 40- and 80-minute time point and ARS+1.6_BC at the 80-minute time point, several common and strong outliers could be detected over the background in the three replicate screens (Figure 2A-C). In total, we identified 85 potential regulators of Pol ε (FDR <0.1 and <-2 fold change). Among the strongest hits for Pol ε depletion were Pol32 (a subunit of replicative Pol δ) (Huang et al., 2002), Dbp4 (a subunit of Pol ε) (Ohya et al., 2000), Mgs1 (Branzei et al., 2002) and the DNA helicase Pif1 (Budd et al., 2006) (Figure 2A-C), all of which are known to play a role in replication. In addition, several mutants were identified in which Pol ε was enriched. However, for this study, we chose to focus on mutants that showed (partial) loss of Pol ε at the barcodes as these may represent mutants with replication fork instability. As expected, mutants with depleted Pol ε were highly enriched in GO terms like "DNA replication" and "DNA repair" (Figure 2D). In addition, a high percentage of mutants with impaired RNAPII transcription were found to have low levels of Pol ε, suggesting that transcription regulation impacts replication (Figure 2D). Next, we performed unbiased hierarchical clustering on ARS_BC (all time points) and ARS+1.6_BC (40- and 80-minute time points), to identify mutants that responded similarly to *pol32Δ* and *dbp4Δ* (Figure 2F). From the resulting clusters, several mutants, including e.g. *YTA7, NSR1 and APT1,* which showed similar Pol ε depletion profiles to *pol32Δ* and *dbp4Δ*, were identified, suggesting that these could be defective in new potential regulators of Pol ε at stalled replication forks (Figure 2E and Table S1). Thus, Repli-ID interrogated Pol ε recruitment near an origin of replication region in nearly 4500 strains simultaneously and identified several new potential regulators of replication fork progression and/or stability.

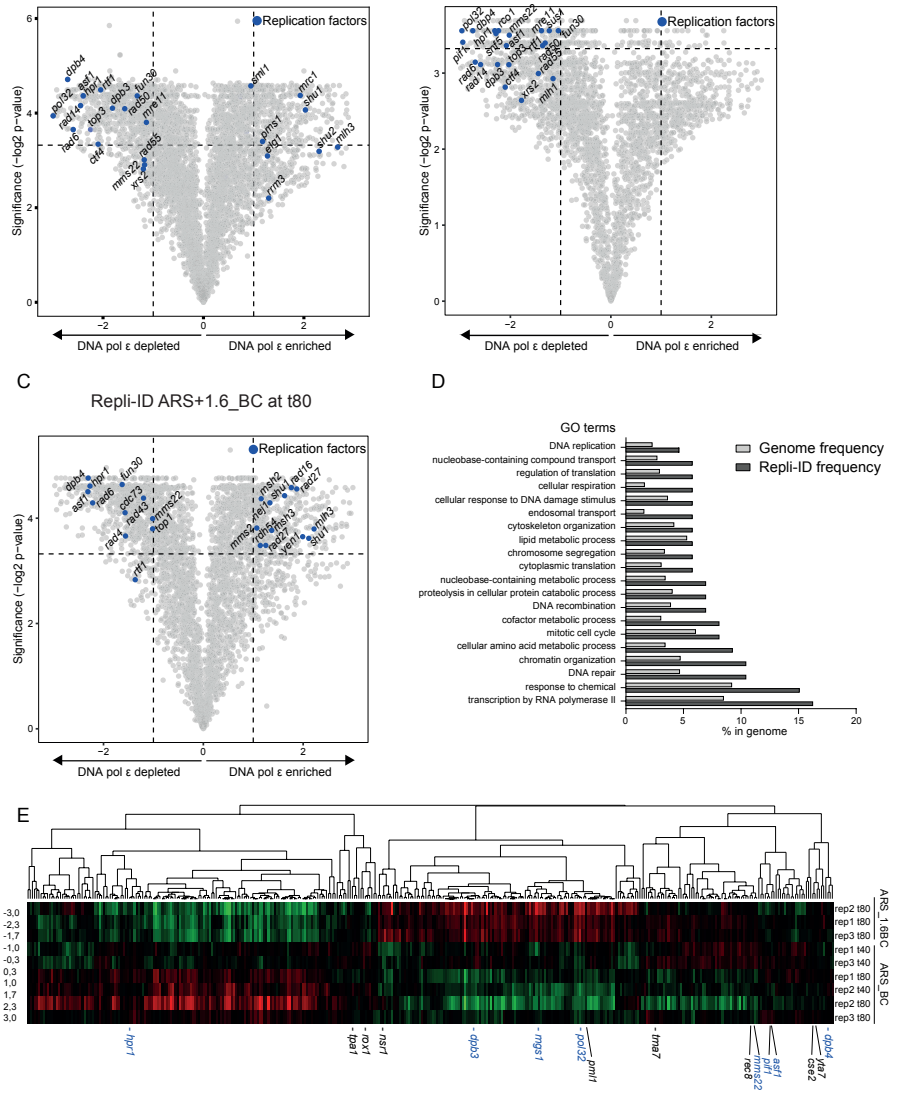

Figure 2. Repli-ID identifies regulators of DNA replication.
Outcome of Repli-ID for Pol e-9xMyc on approximately 4500 strains. Scatter plots show ChIP/Input ratios for (A) ARS_BC at 40 minutes, (B) ARS_BC at 80 minutes and (C) ARS+1.6_BC at 80 minutes. Averages of three independent Repli-ID screens are shown. Each dot represents a single mutant strain. Replication factors showing >2 fold change are highlighted. (D) GO slim analysis of the top 85 factors showing depletion of Pol ε (cut-off <0.1 FDR, >2 fold depletion of Pol ε in at least three ChIPs). Genome frequency is depicted in light grey and frequency within Repli-ID in dark grey. (E) Heatmap of hierarchical clustered data. Genes were selected based on a >2 fold change in Pol ε occupancy in at least one replicate and filtered to keep only those genes showing nuclear localization to filter out proteins located in the cytoplasm. Replication factors are highlighted in blue and factors selected for follow-up in black.

Validation of mutants that affect replication fork stability in Repli-ID screens

To validate results from the Repli-ID screen, we examined Pol e-9xMyc binding near ARS404 and the well-studied early-origin ARS607 (Cobb et al., 2003; Masumoto et al., 2000). Pol e-9xMyc ChIP-qPCR was performed on a selected panel of mutants from the Repli-ID library. These mutants were selected either by significance and effect (FDR <0.1 and >2-fold decreased Pol ε) or by their co-clustering with Pol32 and Dbp4 (Figure 2A-C and E). Confirming findings from the Repli-ID screen, we found that in the majority of selected mutants, namely *yta7Δ*, *tpa1Δ*, *cse2Δ*, *rec8Δ*, *nsr1Δ*, *fpr4Δ*, *rox1Δ*, *egf1Δ*, *med1Δ*, *pml1Δ* and *apt1Δ,* Pol ε levels at ARS404 at 40 minutes were decreased to similar levels as in *pol32Δ*, which served as a positive control (Figure 3A). Importantly, ChIP-qPCR also confirmed Pol ε depletion in these mutants at the early origin ARS607, with the exception of *tpa1Δ*, *med1Δ* and *rec8Δ*.

Next, we investigated by spot dilution assays whether decreased Pol ε levels at replication forks leads to a growth defect after HU treatment. With the exception of *pml1Δ, apt1Δ* and *tma7Δ*, all selected mutants show impaired growth when exposed to HU (Figure 3B). While the loss of *PML1* and *APT1* lead to a severe depletion of Pol ε, this defect, however, did not affect growth on HU. This suggests that Pol ε depletion can be overcome in certain mutants to ensure viability under stress conditions. In conclusion, these results demonstrate that Repli-ID provides a robust and valuable resource for modulators of replication fork stability and/or progression.

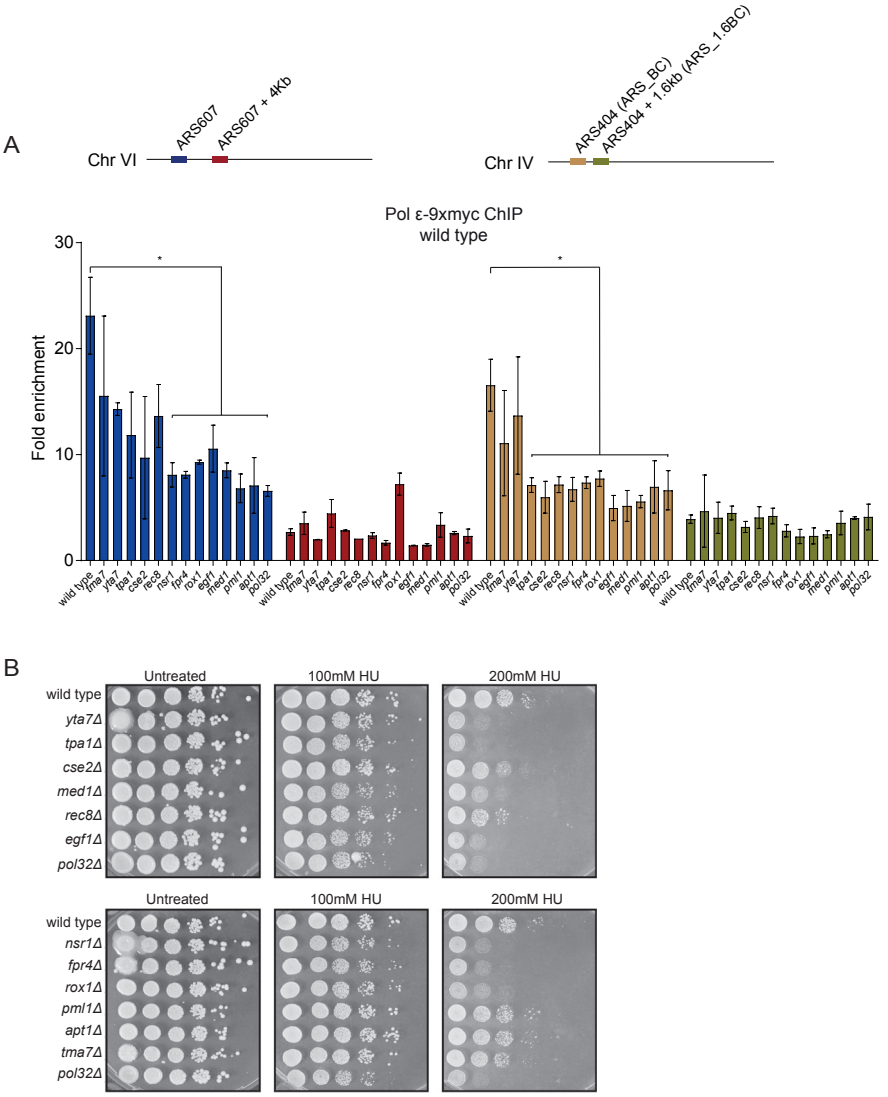

Figure 3. Validation of Repli-ID hits by ChIP-qPCR.
(A) ChIP-qPCR analysis of Pol e-9xMyc at ARS607 and ARS404 for a selection of hits from the Repli-ID screens. Data represent the mean relative fold enrichment of Myc signal over IgG signal in at least three independent experiments ± s.e.m. Values were normalized to ARS607+14kb and compared to wild-type by student T test. (B) Spot dilution assay for a selection of hits from the Repli-ID screens. Cells were diluted and spotted on plates without (untreated) and with the indicated concentrations of HU.

Validation of replication fork instability in *de novo* mutants

Since yeast knock-out libraries can contain incorrect or contaminated mutants (Giaever and Nislow, 2014), we next examined whether Repli-ID hits affect replication fork stability in mutants that were generated *de novo*. To this end, we generated new *nsr1Δ, fpr4Δ, pml1Δ, tpa1Δ* and *rox1Δ* deletion mutants in the W303 background, which is commonly used for replication ChIP assays (Cobb et al., 2003; Franco et al., 2005; Masumoto et al., 2000; Poli et al., 2016; Seeber et al., 2016), yet is distinct from the S288C-derived BY background used in the Repli-ID screens and follow-up experiments. Loss of Nsr1 or Rox1 resulted in low levels of Pol ε at the early-firing origins ARS607 and ARS305 after 20 minutes of release from G1 into S-phase under conditions of HU-induced replication stress (Figure 4A). In contrast, loss of Fpr4, Pml1 and Tpa1 did not show any decrease in Pol ε accumulation (Figure 4A). This may suggest that decreased Pol ε levels in the Repli-ID were not due to the loss of these factors or that their effect on Pol ε is background-dependent.

Nsr1 encodes a nuclear localization sequence-binding protein that is also involved in ribosomal RNA processing (Lee et al., 1991). Rox1 is a highly conserved transcriptional repressor of hypoxic genes containing a nuclear HMG-box domain (Liu and Barrientos, 2013; Lowry and Zitomer, 1988). Since a role for Nsr1 or Rox1 in replication fork stability has not been described, we further investigated by spot dilution assays whether the loss of Nsr1 or Rox1 affects the sensitivity of cells to HU or methyl methanesulfonate (MMS) sensitivity. Loss of Nsr1 resulted in a general growth defect in untreated conditions, as revealed by the formation of seemingly smaller colonies, and did not sensitize cells further to HU. However, loss of Nsr1 moderately increased the sensitivity of cells to MMS (Figure 4B). In contrast, *rox1Δ* displayed a severe growth defect on HU and a modest defect on high concentrations of MMS (Figure 4B). Thus, we identified the Nsr1 and Rox1 as modulators of replication fork progression that protect cells to agents that interfere with DNA replication.

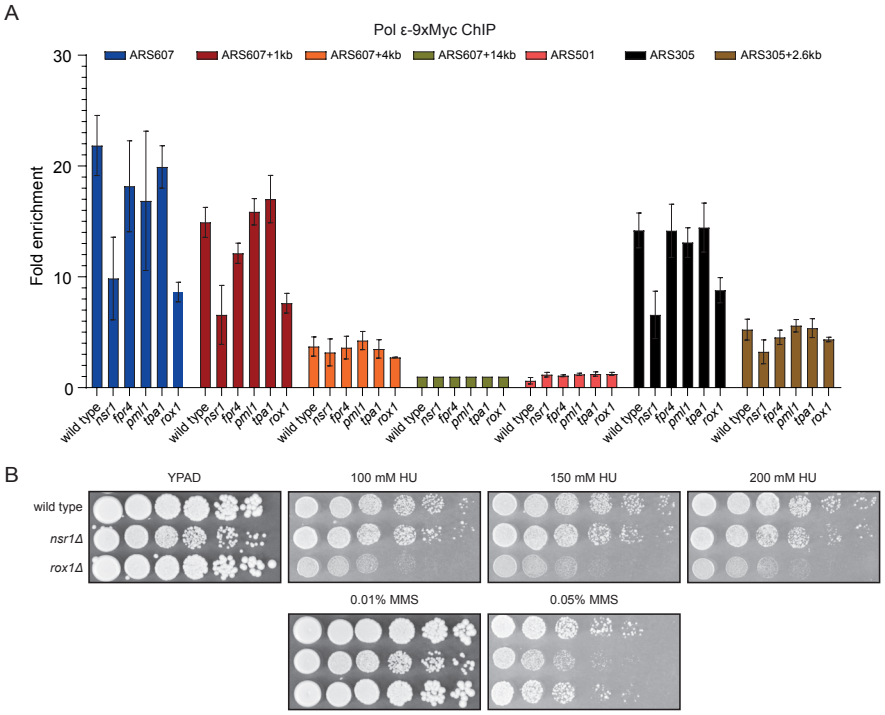

Figure 4. Validation of Repli-ID hits by ChIP-qPCR in *de novo mutants*.
(A) ChIP-qPCR analysis of Pol e-9xMyc at different origins for a selection of hits in *de novo* mutants. Data represent the mean relative fold enrichment of Myc signal over IgG signal in at least three independent experiments ± s.e.m. Values were normalized to unreplicated regions (ARS607+14kb) and compared to wild type by student T test. (B) Spot dilution assay for *nsr1Δ* and *rox1Δ* mutants. Cells were diluted and spotted on plates without (Untreated) and with the indicated concentrations of HU or MMS.

Replication fork progression is affected in *nsr1Δ* and *rox1Δ* mutants

To study how Nsr1 and Rox1 affect DNA replication, we assessed the progression of Pol ε from ARS607 along the chromosome arm at various timepoints in conditions of HU-induced replication stress. In wild-type cells, Pol ε is present at ARS607 20 minutes after entry into S-phase and in the presence of HU. After 40 minutes, Pol ε remains highly enriched up to 2 kb away from the origin and is progressing into the surrounding chromatin after 60 minutes (Figure 5A). Loss of Nsr1 severely affects Pol ε recruitment at 20 minutes after release in S-phase. However, Pol ε loading was partially restored after 40 and 60 minutes and progressed into the surrounding chromatin, suggesting a delay in Pol ε progression (Figure 5B). In contract, loss of Rox1 leads to a striking decrease in the Pol ε levels at all time points, with no delay in progression (Figure 5B). To further assess the effect on DNA replication, we assessed the accumulation of RPA, which coats and protects ssDNA formed

at paused forks (Alani et al., 1992). At 20 minutes after release in S-phase and in the presence of HU, RPA levels were strongly reduced in *nsr1Δ* mutants when compared to wild type (Figure 5C), an effect that was comparable to that of Pol ε (Figure 5C). However, at 60 minutes, *nsr1Δ* mutants accumulated higher levels of RPA than wild-type cells (Figure 5B), whereas Pol ε levels declined (Figure 5C), suggesting that in addition to a delay in replication fork progression, increased fork

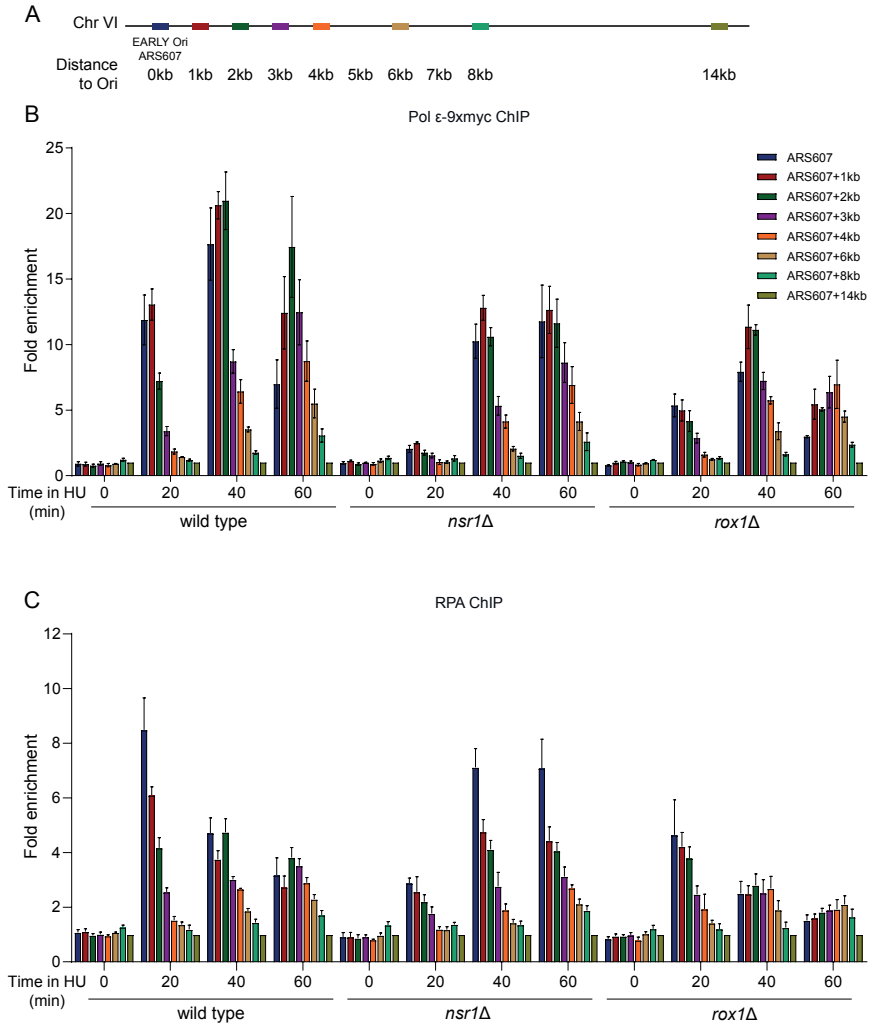

Figure 5. Polymerase ε and RPA profiles at ARS607.
ChIP-qPCR analysis of (A) Pol e-9xMyc and (B) RPA at ARS607 in *nsr1Δ* and *rox1Δ* mutants. Data represent the mean relative fold enrichment of antibody signal over IgG signal in at least three independent experiments ± s.e.m. Values were normalized to unreplicated regions (ARS607+14kb).

stalling and/or instability may occur in the absence of Nsr1. In contrast, RPA levels, similar to Pol ε, were overall decreased in *rox1Δ* mutants, suggesting a defect in the initiation of DNA replication and /or increased fork instability concomitantly with RPA loss (Figure 5B and C).

Loss of Nsr1 results in delayed entry into S-phase

When the entry into S-phase is delayed, this could affect the kinetics of replication fork progression. This may, among others, be caused by an accumulation of cells in G1 phase. Previously, yeast mutants with an increased G1-phase duration were identified (Hoose et al., 2012). We compared these results to our Repli-ID hits to see if these mutants are enriched in the group of Pol ε depleted mutants. Strikingly, we found a significant overrepresentation of mutants with decreased Pol ε in the group of 153 mutants with a prolonged G1-phase, as 25 of them were identified as hits in our Repli-ID screens (Fisher's Exact Test p=3.842e-08), strongly suggesting that the Pol ε reduction in these mutants could be the consequence of altered cell cycle progression. Indeed, *NSR1* was among the mutants showing an increase in G1 phase. To study this further, we profiled the cell cycle of *nsr1Δ,* and included the *rox1Δ* mutant in this analysis. Confirming previous findings, *nsr1Δ* mutants showed an increase in the fraction of G1 cells compared to wild type (Figure 6A). In contrast, cell cycle profiles of *rox1Δ* cells were similar to wild type when grown asynchronously (Figure 6A). Next, we monitored cell cycle progression following an arrest in G1 and release into S-phase in the presence of HU. While wild type cells already progressed into S-phase at 10 minutes after release from G1, *nsr1Δ* cells only showed such a progression by 30 minutes, indicating a delay in S-phase entry (Figure 6A). In contrast, progression into S-phase was comparable between *rox1Δ* and wildtype cells. We therefore conclude that *rox1Δ* mutants progress normally into S-phase, while *nsr1Δ* mutants undergo delayed entry into S-phase.

Ddc2 foci accumulate after HU recovery in *rox1Δ* cells

A failure to recover from replication fork stalling after HU treatment leads to the accumulation of Mec1-Ddc2 in repair foci (Katou et al., 2003; Lisby et al., 2004). To study if loss of Rox1 and Nsr1 results in unrepaired replication forks and checkpoint activation, we examined the formation of Ddc2 foci in these mutants during recovery from replication stress. After 1 hour of HU treatment, cells were released into medium without HU and allowed to recover for 2 hours. Ddc2 foci were observed in approximately 25% of the wild type cells, indicating the presence of stalled/collapsed forks (Figure 6B-C, percentages were normalized to wild-type). While in *nsr1Δ* mutants Ddc2 foci levels were comparable to that in wild type, in *rox1Δ* mutants Ddc2 foci levels were 20% elevated, indicating a failure to properly recover from replication fork stalling

(Figure 6B-C). Therefore, while loss of *NSR1* affects S-phase progression and RPA loading, we do not observe replication fork instability in these mutants. In contrast, loss of Rox1 and the subsequent decrease in the accumulation of Pol ε increases replication fork instability under HU-induced replication stress condition.

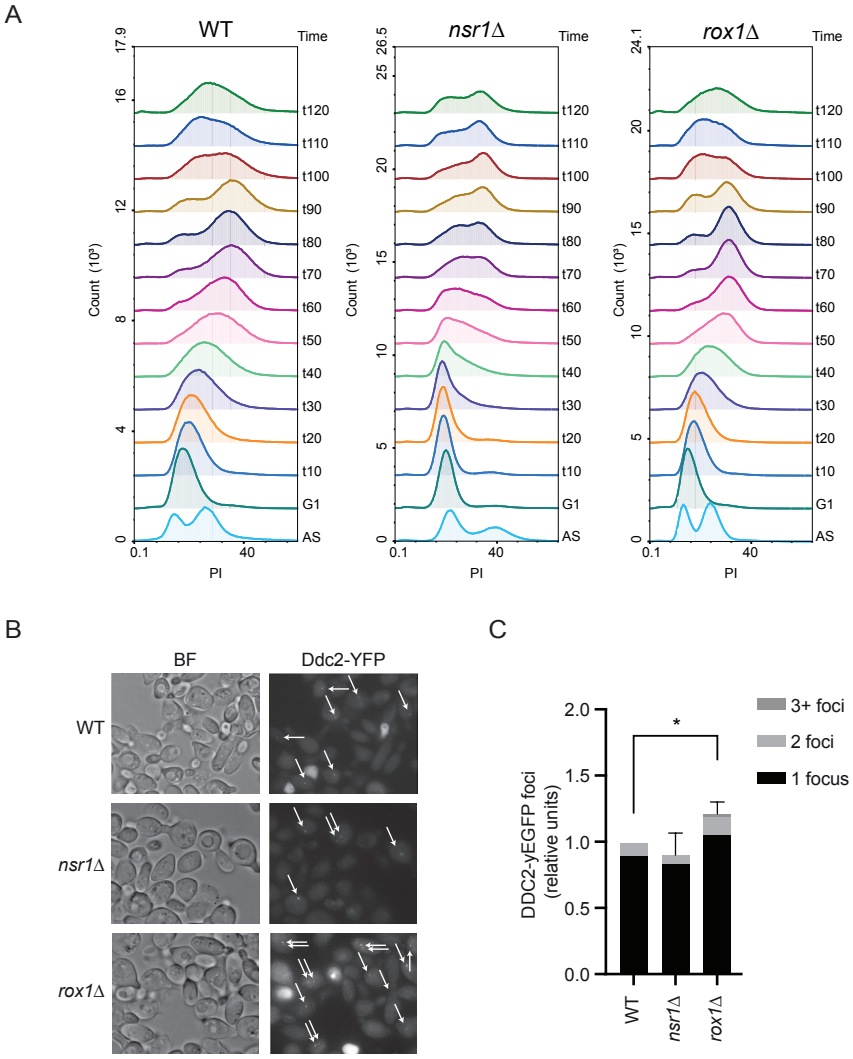

Figure 6. Cell cycle profiles and Ddc2 foci formation in *nsr1Δ* and *rox1Δ* mutants.
(A) FACS analysis of cell cycle profiles in *nsr1Δ* and *rox1Δ* mutants. Mutants were grown, arrested in G1 and released in 10mM of HU to profile cell cycle progression. (B) Ddc2-YFP foci formation was scored after treating *nsr1Δ* and *rox1Δ* mutants with HU and letting them recover for 2 hours. BF = brightfield.

DISCUSSION

Here, we present a new technology called Repli-ID to study replication fork stability and progression. By examining the enrichment of Pol ε at a barcoded origin of replication, ARS404, in a large collection of yeast deletion strains, we uncovered genes that modulate Pol ε progression and/or stability. The most striking hits were genes that encode subunits of the replicative polymerases δ and ε (Pol32 and Dbp4) and the Pif1 helicase, showing the validity of the approach. In addition, we also identified 85 other potential regulators of Pol ε. Thus, Repli-ID generated a comprehensive view of mutants affecting Pol ε in yeast and provides a resource for follow-up studies that aim to understand the biological role of these factors in replication.

In addition to mutants with decreased Pol ε levels, we also identified many mutants with increased Pol ε occupancy at ARS404. High occupancy by Pol ε has been used as a measure for the identification of sites where replication forks move more slowly than elsewhere in the genome (Azvolinsky et al., 2009). These sites are mostly found at ribosomal gene (rDNA) repeats, telomeric regions, centromeres, tRNA genes or inactive replication origins (Ivessa et al., 2003). Moreover, head-on collisions between the RNAPII machinery and the replication fork coming from ARS404 might also increase fork pausing, leading to increased Pol ε during Repli-ID. More follow-up research is required to study how loss of certain factors leads to increased Pol ε near origins of replication and what the cellular consequences are.

Initial validation experiments using strains from the Repli-ID library showed that mutants affecting Pol ε recruitment at ARS404 also affected Pol ε recruitment at early origin ARS607, suggesting that most mutants have a general effect on replication fork progression and/or stability. However, *de novo* mutants in W303 background indicated background or library effects can influence Pol ε at stalled forks, as shown for *fpr4Δ, pml1Δ* and *tpa1Δ*. Large-scale background effects were also observed in the transcriptional response to HU: while in the S288C background 1,735 genes displayed a two-fold change in gene expression, the common changes between S288C and W303 were limited to only 126 genes (Dubacq et al., 2006). Thus, further validation of hits from the Repli-ID screen in different yeast backgrounds is critical prior to further follow-up studies.

Factors involved in RNAPII transcription were overrepresented among those that affecting Pol ε at ARS404, suggesting a link between transcription regulation and replication fork progression and/or stability. Indeed, transcription-replication conflicts are known to cause DNA replication fork stalling and pose a source for DNA damage. Moreover, head-on collisions between the transcription and replication machineries have been shown to lead to recombination events (Prado and Aguilera, 2005). These events may involve the formation of R-loops, which can arise as a consequence of

misregulated transcription. Various transcriptional regulators, such as the prefoldin protein Bud27, the transcription factors Hap2 and Hap4, and the Mediator subunits Cse2 and Med1, were overrepresented in the pool of mutants affecting Pol ε recruitment. Understanding how they affect polymerase recruitment could further decipher the link between DNA replication and transcription.

Another subset of factors with decreased Pol ε was enriched for mutants with altered cell cycle progression (Hoose et al., 2012). This correlation could imply that Pol ε recruitment can be affected indirectly through the regulation of S-phase entry or origin firing. Repli-ID cannot distinguish between delayed S-phase entry and replication fork instability in mutants, since both can result in decreased Pol ε at origins of replication. However, we can identify mutants with delayed S-phase entry by FACS or by investigating the levels of RPA or Cdc45-Mcm2-7-GINS (CMG) helicase at origins since a decrease in origin firing or unwinding directly relates to the loading of these factors (Fang et al., 2016; Tanaka and Nasmyth, 1998). Performing Repli-ID with factors other than Pol ε, such as RPA or the CMG helicase could provide insight into mutants that experience delayed S-phase entry or delayed origin firing.

Follow-up from Repli-ID screens identified Nsr1 as a regulator of DNA replication. Loss of Nsr1 results in delayed progression of Pol ε and decreased RPA loading in response to HU. Loss of RPA can be both associated with delayed origin firing or replication fork collapse (Tanaka and Nasmyth, 1998). However, the restoration of RPA at later timepoints in *nsr1Δ* indicates delayed origin firing, which was corroborated by delayed entry into S-phase of *nsr1Δ* cells (Azevedo et al., 2015). Therefore, the decreased levels of Pol ε in *nsr1Δ* mutants is likely due to delayed S-phase entry, since there is no indication of replication fork instability in these mutants.

Our Repli-ID screens and follow-up in *de novo* constructed strains also identified that loss of Rox1 impairs replication fork progression and causes replication stress. As a transcriptional repressor, Rox1 regulates the expression of around 100 genes (Kwast et al., 2002). However, most of these genes have not been implicated in DNA replication, but have roles in respiration, cell wall composition and sterol and heme biosynthesis, except for the *RNR* genes, which control the supply of dNTPs (Klinkenberg et al., 2006). Specifically, Rox1 has been implicated in regulating transcription of *RNR3-4,* but not *RNR1* (Klinkenberg et al., 2006), and as such may control dNTPs levels. Elevated dNTP levels have been associated with accelerated fork progression, decreased fidelity of replicative polymerases and decreased efficiency of mismatch repair (Buckland et al., 2014; Poli et al., 2012; Schmidt et al., 2019). Although, loss of Rox1 neither affected the progression of cells from G1 into S-phase, nor impacted cell cycle profiles, increased dNTP levels may affect the balance between Pol ε and translesion synthesis polymerases, since they have a higher affinity for dNTPs than Pol ε (Lis et al., 2008; Sabouri et al., 2008). As such, higher dNTPs

levels could induce a switch from Pol ε to error-prone translesion synthesis polymerases, resulting in decreased level of Pol ε at replication forks in *rox1Δ* mutants. Consequently, *rox1Δ* mutants may suffer from elevated mutagenesis, which could be validated using mutational reporters, such as for instance the *CAN1* gene, in which TLS-induced mutations give rise to canavanine resistance.

Currently, Repli-ID is performed with the overexpression of Sld3-Dbf4 mutants to fire ARS404 in early S-phase. To alleviate the need for firing all origins simultaneously, a possibility is to redesign the barcoder library with CRISPR/Cas9 and place all barcodes near the early-firing origin ARS607 (Korthout et al., 2018). With such a redesign, barcodes could also be distributed across a longer distance near the origin of replication to provide more information into the regulation of replication forks in space and time in WT cells, independent of the overexpression of Sld3-Dbf4. On the other hand, Repli-ID can be performed in other configurations than by using tagged a replicative polymerase. For instance, by performing Repli-ID screens with tagged Rad51, mutants in which loss of Pol ε leads to collapsed forks and initiation of homologous recombination may be identified. Alternatively, interrogating the Rad18 status at stalled replication forks during Repli-ID may reveal novel regulators of DNA damage tolerance pathways. These examples illustrate the applicability of the Repli-ID approach to further interrogate the factors and mechanisms involved in replication fork maintenance.

MATERIALS AND METHODS

Yeast strains, plasmids and antibodies

Yeast strains and plasmids used in this study are listed in Table 1 and 2. Yeast strains that were used in the initial Repli-ID validation studies were taken from the yeast knockout (YKO) library (Tong and Boone, 2006) and verified by PCR and phenotypic analysis. Yeast libraries were crossed using a RoToR from Singer Instruments and synthetic genetic array (SGA) technology (Tong and Boone, 2006). Antibodies used were anti-myc 9B11 (#2276, Cell Signaling, Leiden, the Netherlands), anti-flag (anti-Pgk1 (#459250; Invitrogen, Carlsbad, CA), anti-H4 (ab10158; Abcam, Cambridge, UK) and anti-H3 (ab1791; Abcam).

Repli-ID screen

Repli-ID was performed based on (Vlaming et al., 2016). Briefly, the collection of barcoded yeast mutants was generated by crossing 1140 barcoder strains (Yan et al., 2008) to the *MAT*α NatMX knock-out (Tong and Boone, 2006) of yeast mutants. Deletion mutants were divided over 5 subsets of unique barcodes and a wild-type barcode set as a control. Next, the strain

containing myc-tagged Pol ε (Pol e-9xMyc) and the SLD3/DBF4 mutant overexpression construct (adapted from (Zegerman and Diffley, 2010)) integrated at BAR1 locus were crossed into barcoded libraries to generate the Repli-ID library. Library plates were grown overnight on plates containing raffinose. In the morning, they were diluted to 0.1 OD and grown for 3 hours in rich medium containing raffinose. To arrest the cells in G1, α-factor was added for 2.5 hours with extra additions after 1 hour and after 2 hours. During the last 30 minutes of α-factor arrest, galactose was added to induce expression of the SLD3/DBF4 mutant construct and subsequently fire all origins during release into S-phase. Before release in S-phase, a fraction was crosslinked for ChIP at the t0 timepoint. α-factor was removed by washing the yeast twice in YPAD and released into YPAD containing 0.2M HU (Sigma-Aldrich) and pronase (Merck Millipore). Samples were crosslinked after 40 and 80 minutes. ChIP and library prep was performed as in (Vlaming et al., 2016), except that ChIP was performed using the anti-myc antibody. Deep-sequencing was performed on a single-end flow-cell Illumina Hi-Seq2500.

Repli-ID analysis

Barcodes were counted and depletion or enrichment of a barcode was scored as in (Vlaming et al., 2016). Unsupervised cluster was performed using Cluster 3.0, on genes with a score of > -1.5 in at and with FDR value of < 0.1. The clustering was visualized in a heatmap using Java TreeView.

Spot dilution test

Cells were grown to mid-log in rich media (YPAD) collected and set to concentration of 2.5 x 10^8/ml, 10-fold serial dilutions were generated and spotted on plate containing rich YPAD and YPAD containing 50 mM and 100 mM HU and were grown for 3 days respectively at 30 ˚C.

Ddc2 focus formation assay

Cell containing endogenously tagged Ddc2-GFP were grown to mid-log, synchronized with YPAD containing α-factor for 2 hours, washed and released in YPAD containing 0.2 M HU (Sigma-Aldrich) for 1 hour, after which cells were allowed to recover in YPAD for 2h. Cells were collected and fixed in 4% paraformaldehyde at room temperature for 15 minutes, washed and resuspended in KPO4/Sorbitol solution (10 mM KPO4, 1.2 M Sorbitol, pH=7.5). Images were captured with a Zeiss AxioImager M2 widefield fluorescence microscope equipped with 100x PLAN APO (1.4 NA) oil-immersion objectives (Zeiss) and an HXP 120 metal-halide lamp used for excitation. 21 focal steps of 0.25µm were acquired with an exposure time of 1000 ms using a GFP/YFP 488 filter (excitation filter: 470/40 nm, dichroic mirror: 495 nm, emission filter: 525/50 nm). Images were recorded using ZEN 2012 software and analyzed with Fiji.

ChIP-qPCR

ChIP was performed as previously described (Cobb and van Attikum, 2010). Briefly, for Repli-ID validation the ChIP protocol from the Repli-ID screen was used. For *de novo* generated strains in W303 background, cells were grown for 3 hours, treated with α-factor for 2 hours, washed once in YPAD medium and released in YPAD containing 0.2M HU. Samples were collected at 0, 20, 40 and 60 minutes after release and fixed with 1 % formaldehyde. Input and immunoprecipitated DNA was purified and analyzed by quantitative (q)PCR using primers listed in Table 2. Relative enrichment was determined by 2-DDCt method. Signal for Dynabeads alone was used to correct for background.

Western blot analysis

Whole cell extracts were prepared from approximately 2.5 x10^7 cells. Cell pellets were incubated for 10 minutes in 1.85N NaOH and 7.4% β-mercaptoethanol, followed by precipitation with trichloracetic acid (TCA). Samples were dissolved and boiled in SDS–PAGE sample. Proteins were resolved in 12% polyacrylamide gels and transferred onto PDVF membranes. Membranes were blocked with blocking buffer (Rockland) in PBS followed by overnight incubation with primary antibody in blocking buffer at 4˚C. Membranes were washed with 0.1% Tween20 in PBS. Secondary antibody incubations were performed for 60 minutes in blocking buffer at room temperature using LI-COR® Odyssey IRDye® 800CW (1:10.000). Membranes were subsequently scanned on a LI-COR Odyssey® IR Imager (Biosciences).

Flow Cytometry

Overnight cultures were grown to mid-log, synchronized with YPAD containing α-factor for 2 hours, washed and released in YPAD containing 10mM HU. Aliquots of cells were collected and fixed in 70% cold ethanol at specified time intervals. After overnight fixation, cells were incubated with 200 μg/ml RNAse A at 37°C for 3 h. Cells were resuspended and PI was added to a final concentration of 10 μg/ml. Cells were briefly sonicated, after which 250.000 events were recorded on a Novocyte (ACEA Biosciences, Inc) and analyzed with NovoExpress software.

Statistical analysis

To calculate the enrichment of yeast mutants with an increased G1-phase duration (Hoose et al., 2012) in the Repli-ID results, a Fisher's Exact Test for Count Data was performed.

AUTHOR CONTRIBUTIONS

L.K. performed the Repli-ID screens and analysis, ChIP-qPCR, FACS and microscopic experiments, and wrote the paper. A.B. performed the Repli-ID screens, ChIP-qPCR, FACS and microscopic experiments. S.v.d.H. performed FACS, ChIP-qPCR and microscopic experiments. H.v.A. supervised the project and wrote the paper.

ACKNOWLEDGEMENTS

This work was financially supported by ERC-CoG (617485) and NWO-Vici (182.052) grants to H.v.A..

Table 1 - Yeast strains

Name	Genotype	Reference
yHA-269 Pol ε-MYC	*MAT*a *ade2-1 trp1-1 his3-11 his3-15 ura3-1 leu2-3 leu2-112 RAD5-(W303)* *POLe-9xMYC::KanMX bar1Δ::NatMX*	This study
yHA-1167 *nsr1Δ*	Isogenic to yHA-269 except *nsr1Δ::HIS3*	This study
yHA-1168 *fpr4Δ*	Isogenic to yHA-269 except *fpr4Δ::HIS3*	This study
yHA-1169 *pml1Δ*	Isogenic to yHA-269 except *pml1Δ::HIS3*	This study
yHA-1170 *pml1Δ*	Isogenic to yHA-269 except *pml1Δ::HIS3*	This study
yHA-1171 *rox1Δ*	Isogenic to yHA-269 except *rox1Δ::HIS3*	This study
yHA-265	*MAT*a ade2-1 trp1-1 his3-11 his3-15 ura3-1 leu2-3 leu2-112 *RAD5*+ (W303) *bar1Δ::LEU2 DDC2-YFP*	(Lisby et al., 2004)
yHA-1242 *nsr1Δ*	Isogenic to yHA-265 except *nsr1Δ::HIS3*	This study
yHA-1243 *rox1Δ*	Isogenic to yHA-265 except *rox11Δ::HIS3*	This study

Table 2 – qPCR Primers

Target	Sequence
ARS607 ChIP-qPCR F	CTTTAGCTGGGTTTATGGGAGGTT
ARS607 ChIP-qPCR R	TAATGCACGAGCCGAAACAA
ARS607+1kb ChIP-qPCR F	GGAGAGAATCTTACCTCAGAGTGC
ARS607+1kb ChIP-qPCR R	GGGATCTTGAAAGTAAAACAGGTG
ARS607+2kb ChIP-qPCR F	CGCAGCAGTGGAGTTATCAG
ARS607+2kb ChIP-qPCR R	TAATCCACTTTGTCGGGCCA
ARS607+3kb ChIP-qPCR F	CTTTGTTATGGACCCGGAGA
ARS607+3kb ChIP-qPCR R	CATCAAGATGGAATACTGTGACAA
ARS607+4kb ChIP-qPCR F	TATGCTATCGTCGAGATGTTGTTCT
ARS607+4kb ChIP-qPCR R	GGTGGAAGCGCAGGTTGATC
ARS607+6kb ChIP-qPCR F	GTTTCACCTCGTAGTCCCTCA
ARS607+6kb ChIP-qPCR R	AACCAAATGCATTGCTTTATCA
ARS607+14kb ChIP-qPCR F	CAGGATATGCGGCCAAATTT
ARS607+14kb ChIP-qPCR R	GCATGACAGCCGAATCGAT
ARS501 ChIP-qPCR F	AAGCAAATTGCAGAAGGTTATGAA
ARS501 ChIP-qPCR R	TTCAAGGCTCTAGCATATGAAACG
ARS305 ChIP-qPCR F	CGCCCGACGCCGTAA
ARS305 ChIP-qPCR R	GAGCGGCCTGAAATACTGTCA
ARS305+2.6kb ChIP-qPCR F	CAAAGGTCGGCTGCTTCAAT
ARS305+2.6kb ChIP-qPCR R	GGTATAGGCCAGGGAAGAAGGT

REFERENCES

1. Alani, E., Thresher, R., Griffith, J.D., and Kolodner, R.D. (1992). Characterization of DNA-binding and strand-exchange stimulation properties of y-RPA, a yeast single-strand-DNA-binding protein. Journal of molecular biology *227*, 54-71.

2. Alcasabas, A.A., Osborn, A.J., Bachant, J., Hu, F., Werler, P.J., Bousset, K., Furuya, K., Diffley, J.F., Carr, A.M., and Elledge, S.J. (2001). Mrc1 transduces signals of DNA replication stress to activate Rad53. Nature cell biology *3*, 958-965.

3. Azevedo, C., Livermore, T., and Saiardi, A. (2015). Protein polyphosphorylation of lysine residues by inorganic polyphosphate. Mol Cell *58*, 71-82.

4. Azvolinsky, A., Giresi, P.G., Lieb, J.D., and Zakian, V.A. (2009). Highly transcribed RNA polymerase II genes are impediments to replication fork progression in Saccharomyces cerevisiae. Mol Cell *34*, 722-734.

5. Bando, M., Katou, Y., Komata, M., Tanaka, H., Itoh, T., Sutani, T., and Shirahige, K. (2009). Csm3, Tof1, and Mrc1 form a heterotrimeric mediator complex that associates with DNA replication forks. J Biol Chem *284*, 34355-34365.

6. Bjergbaek, L., Cobb, J.A., Tsai-Pflugfelder, M., and Gasser, S.M. (2005). Mechanistically distinct roles for Sgs1p in checkpoint activation and replication fork maintenance. The EMBO journal *24*, 405-417.

7. Branzei, D., and Foiani, M. (2009). The checkpoint response to replication stress. DNA Repair (Amst) *8*, 1038-1046.

8. Branzei, D., Seki, M., Onoda, F., and Enomoto, T. (2002). The product of Saccharomyces cerevisiae WHIP/MGS1, a gene related to replication factor C genes, interacts functionally with DNA polymerase delta. Molecular genetics and genomics : MGG *268*, 371-386.

9. Buckland, R.J., Watt, D.L., Chittoor, B., Nilsson, A.K., Kunkel, T.A., and Chabes, A. (2014). Increased and imbalanced dNTP pools symmetrically promote both leading and lagging strand replication infidelity. PLoS Genet *10*, e1004846.

10. Budd, M.E., Reis, C.C., Smith, S., Myung, K., and Campbell, J.L. (2006). Evidence suggesting that Pif1 helicase functions in DNA replication with the Dna2 helicase/nuclease and DNA polymerase delta. Mol Cell Biol *26*, 2490-2500.

11. Cejka, P., Cannavo, E., Polaczek, P., Masuda-Sasa, T., Pokharel, S., Campbell, J.L., and Kowalczykowski, S.C. (2010). DNA end resection by Dna2-Sgs1-RPA and its stimulation by Top3-Rmi1 and Mre11-Rad50-Xrs2. Nature *467*, 112-116.

12. Chabes, A., Georgieva, B., Domkin, V., Zhao, X., Rothstein, R., and Thelander, L. (2003). Survival of DNA damage in yeast directly depends on increased dNTP levels allowed by relaxed feedback inhibition of ribonucleotide reductase. Cell *112*, 391-401.

13. Chang, M., Bellaoui, M., Boone, C., and Brown, G.W. (2002). A genome-wide screen for methyl methanesulfonate-sensitive mutants reveals genes required for S phase progression in the presence of DNA damage. Proceedings of the National Academy of Sciences of the United States of America *99*, 16934-16939.

14. Cobb, J., and van Attikum, H. (2010). Mapping genomic targets of DNA helicases by chromatin immunoprecipitation in Saccharomyces cerevisiae. Methods in molecular biology (Clifton, NJ) *587*, 113-126.

15. Cobb, J.A., Bjergbaek, L., Shimada, K., Frei, C., and Gasser, S.M. (2003). DNA polymerase stabilization at stalled replication forks requires Mec1 and the RecQ helicase Sgs1. Embo j *22*, 4325-4336.

16. Dubacq, C., Chevalier, A., Courbeyrette, R., Petat, C., Gidrol, X., and Mann, C. (2006). Role of the iron mobilization and oxidative stress regulons in the genomic response of yeast to hydroxyurea. Molecular genetics and genomics : MGG *275*, 114-124.

17. Fang, D., Cao, Q., and Lou, H. (2016). Sld3-MCM Interaction Facilitated by Dbf4-Dependent Kinase Defines an Essential Step in Eukaryotic DNA Replication Initiation. Frontiers in microbiology *7*, 885.

18. Franco, A.A., Lam, W.M., Burgers, P.M., and Kaufman, P.D. (2005). Histone deposition protein Asf1 maintains DNA replisome integrity and interacts with replication factor C. Genes & development *19*, 1365-1375.

19. Gaillard, H., Garcia-Muse, T., and Aguilera, A. (2015). Replication stress and cancer. Nature reviews Cancer *15*, 276-289.

20. Giaever, G., and Nislow, C. (2014). The yeast deletion collection: a decade of functional genomics. Genetics *197*, 451-465.

21. Hartman, J.L.t., and Tippery, N.P. (2004). Systematic quantification of gene interactions by phenotypic array analysis. Genome Biol *5*, R49.

22. Hegnauer, A.M., Hustedt, N., Shimada, K., Pike, B.L., Vogel, M., Amsler, P., Rubin, S.M., van Leeuwen, F., Guénolé, A., van Attikum, H., *et al.* (2012). An N-terminal acidic region of Sgs1 interacts with Rpa70 and recruits Rad53 kinase to stalled forks. The EMBO journal *31*, 3768-3783.

23. Hoose, S.A., Rawlings, J.A., Kelly, M.M., Leitch, M.C., Ababneh, Q.O., Robles, J.P., Taylor, D., Hoover, E.M., Hailu, B., McEnery, K.A., *et al.* (2012). A systematic analysis of cell cycle regulators in yeast reveals that most factors act independently of cell size to control initiation of division. PLoS Genet *8*, e1002590.

24. Huang, M.E., Rio, A.G., Galibert, M.D., and Galibert, F. (2002). Pol32, a subunit of Saccharomyces cerevisiae DNA polymerase delta, suppresses genomic deletions and is involved in the mutagenic bypass pathway. Genetics *160*, 1409-1422.

25. Ivessa, A.S., Lenzmeier, B.A., Bessler, J.B., Goudsouzian, L.K., Schnakenberg, S.L., and Zakian, V.A. (2003). The Saccharomyces cerevisiae helicase Rrm3p facilitates replication past nonhistone protein-DNA complexes. Mol Cell *12*, 1525-1536.

26. Katou, Y., Kanoh, Y., Bando, M., Noguchi, H., Tanaka, H., Ashikari, T., Sugimoto, K., and Shirahige, K. (2003). S-phase checkpoint proteins Tof1 and Mrc1 form a stable replication-pausing complex. Nature *424*, 1078-1083.

27. Kim, S., and Weinert, T.A. (1997). Characterization of the checkpoint gene RAD53/MEC2 in Saccharomyces cerevisiae. Yeast *13*, 735-745.

28. Klinkenberg, L.G., Webb, T., and Zitomer, R.S. (2006). Synergy among differentially regulated repressors of the ribonucleotide diphosphate reductase genes of Saccharomyces cerevisiae. Eukaryot Cell *5*, 1007-1017.

29. Korthout, T., Poramba-Liyanage, D.W., van Kruijsbergen, I., Verzijlbergen, K.F., van Gemert, F.P.A., van Welsem, T., and van Leeuwen, F. (2018). Decoding the chromatin proteome of a single genomic locus by DNA sequencing. PLoS biology *16*, e2005542.

30. Kwast, K.E., Lai, L.C., Menda, N., James, D.T., 3rd, Aref, S., and Burke, P.V. (2002). Genomic analyses of anaerobically induced genes in Saccharomyces cerevisiae: functional roles of Rox1 and other factors in mediating the anoxic response. J Bacteriol *184*, 250-265.

31. Lee, W.C., Xue, Z.X., and Melese, T. (1991). The NSR1 gene encodes a protein that specifically binds nuclear localization sequences and has two RNA recognition motifs. J Cell Biol *113*, 1-12.

32. Lis, E.T., O'Neill, B.M., Gil-Lamaignere, C., Chin, J.K., and Romesberg, F.E. (2008). Identification of pathways controlling DNA damage induced mutation in Saccharomyces cerevisiae. DNA Repair (Amst) *7*, 801-810.

33. Lisby, M., Barlow, J.H., Burgess, R.C., and Rothstein, R. (2004). Choreography of the DNA damage response: spatiotemporal relationships among checkpoint and repair proteins. Cell *118*, 699-713.

34. Liu, J., and Barrientos, A. (2013). Transcriptional regulation of yeast oxidative phosphorylation hypoxic genes by oxidative stress. Antioxidants & redox signaling *19*, 1916-1927.

35. Lopez-Mosqueda, J., Maas, N.L., Jonsson, Z.O., Defazio-Eli, L.G., Wohlschlegel, J., and Toczyski, D.P. (2010). Damage-induced phosphorylation of Sld3 is important to block late origin firing. Nature *467*, 479-483.

36. Lowry, C.V., and Zitomer, R.S. (1988). ROX1 encodes a heme-induced repression factor regulating ANB1 and CYC7 of Saccharomyces cerevisiae. Mol Cell Biol *8*, 4651-4658.

37. Majka, J., and Burgers, P.M. (2003). Yeast Rad17/Mec3/Ddc1: a sliding clamp for the DNA damage checkpoint. Proc Natl Acad Sci U S A *100*, 2249-2254.

38. Masumoto, H., Sugino, A., and Araki, H. (2000). Dpb11 controls the association between DNA polymerases alpha and epsilon and the autonomously replicating sequence region of budding yeast. Mol Cell Biol *20*, 2809-2817.

39. Morafraile, E.C., Diffley, J.F., Tercero, J.A., and Segurado, M. (2015). Checkpoint-dependent RNR induction promotes fork restart after replicative stress. Sci Rep *5*, 7886.

40. Mordes, D.A., Nam, E.A., and Cortez, D. (2008). Dpb11 activates the Mec1-Ddc2 complex. Proceedings of the National Academy of Sciences of the United States of America *105*, 18730-18734.

41. Ohya, T., Maki, S., Kawasaki, Y., and Sugino, A. (2000). Structure and function of the fourth subunit (Dpb4p) of DNA polymerase epsilon in Saccharomyces cerevisiae. Nucleic Acids Res *28*, 3846-3852.

42. Osborn, A.J., and Elledge, S.J. (2003). Mrc1 is a replication fork component whose phosphorylation in response to DNA replication stress activates Rad53. Genes & development *17*, 1755-1767.

43. Paciotti, V., Lucchini, G., Plevani, P., and Longhese, M.P. (1998). Mec1p is essential for phosphorylation of the yeast DNA damage checkpoint protein Ddc1p, which physically interacts with Mec3p. The EMBO journal *17*, 4199-4209.

44. Pardo, B., Crabbe, L., and Pasero, P. (2017). Signaling pathways of replication stress in yeast. FEMS yeast research *17*.

45. Parsons, A.B., Lopez, A., Givoni, I.E., Williams, D.E., Gray, C.A., Porter, J., Chua, G., Sopko, R., Brost, R.L., Ho, C.H., *et al.* (2006). Exploring the mode-of-action of bioactive compounds by chemical-genetic profiling in yeast. Cell *126*, 611-625.

46. Poli, J., Gerhold, C.-B., Tosi, A., Hustedt, N., Seeber, A., Sack, R., Herzog, F., Pasero, P., Shimada, K., Hopfner, K.-P., *et al.* (2016). Mec1, INO80, and the PAF1 complex cooperate to limit transcription replication conflicts through RNAPII removal during replication stress. Genes & development *30*, 337-354.

47. Poli, J., Tsaponina, O., Crabbe, L., Keszthelyi, A., Pantesco, V., Chabes, A., Lengronne, A., and Pasero, P. (2012). dNTP pools determine fork progression and origin usage under replication stress. Embo j *31*, 883-894.

48. Prado, F., and Aguilera, A. (2005). Impairment of replication fork progression mediates RNA polII transcription-associated recombination. Embo j *24*, 1267-1276.

49. Puddu, F., Granata, M., Di Nola, L., Balestrini, A., Piergiovanni, G., Lazzaro, F., Giannattasio, M., Plevani, P., and Muzi-Falconi, M. (2008). Phosphorylation of the budding yeast 9-1-1 complex is required for Dpb11 function in the full activation of the UV-induced DNA damage checkpoint. Molecular and cellular biology *28*, 4782-4793.

50. Rouse, J., and Jackson, S.P. (2002). Lcd1p recruits Mec1p to DNA lesions in vitro and in vivo. Molecular cell *9*, 857-869.

51. Sabouri, N., Viberg, J., Goyal, D.K., Johansson, E., and Chabes, A. (2008). Evidence for lesion bypass by yeast replicative DNA polymerases during DNA damage. Nucleic Acids Res *36*, 5660-5667.

52. Schmidt, T.T., Sharma, S., Reyes, G.X., Gries, K., Gross, M., Zhao, B., Yuan, J.H., Wade, R., Chabes, A., and Hombauer, H. (2019). A genetic screen pinpoints ribonucleotide reductase residues that sustain dNTP homeostasis and specifies a highly mutagenic type of dNTP imbalance. Nucleic Acids Res *47*, 237-252.

53. Seeber, A., Hegnauer, A.M., Hustedt, N., Deshpande, I., Poli, J., Eglinger, J., Pasero, P., Gut, H., Shinohara, M., Hopfner, K.-P*., et al.* (2016). RPA Mediates Recruitment of MRX to Forks and Double-Strand Breaks to Hold Sister Chromatids Together. Molecular cell *64*, 951-966.

54. Sogo, J.M., Lopes, M., and Foiani, M. (2002). Fork reversal and ssDNA accumulation at stalled replication forks owing to checkpoint defects. Science *297*, 599-602.

55. Tanaka, K., and Russell, P. (2001). Mrc1 channels the DNA replication arrest signal to checkpoint kinase Cds1. Nature cell biology *3*, 966-972.

56. Tanaka, T., and Nasmyth, K. (1998). Association of RPA with chromosomal replication origins requires an Mcm protein, and is regulated by Rad53, and cyclin- and Dbf4-dependent kinases. Embo j *17*, 5182-5191.

57. Tercero, J.A., and Diffley, J.F. (2001). Regulation of DNA replication fork progression through damaged DNA by the Mec1/Rad53 checkpoint. Nature *412*, 553-557.

58. Tong, A.H., and Boone, C. (2006). Synthetic genetic array analysis in Saccharomyces cerevisiae. Methods in molecular biology (Clifton, NJ) *313*, 171-192.

59. Travesa, A., Kuo, D., de Bruin, R.A., Kalashnikova, T.I., Guaderrama, M., Thai, K., Aslanian, A., Smolka, M.B., Yates, J.R., 3rd, Ideker, T*., et al.* (2012). DNA replication stress differentially regulates G1/S genes via Rad53-dependent inactivation of Nrm1. Embo j *31*, 1811-1822.

60. Tsai, F.L., Vijayraghavan, S., Prinz, J., MacAlpine, H.K., MacAlpine, D.M., and Schwacha, A. (2015). Mcm2-7 Is an Active Player in the DNA Replication Checkpoint Signaling Cascade via Proposed Modulation of Its DNA Gate. Mol Cell Biol *35*, 2131-2143.

61. Vlaming, H., Molenaar, T.M., van Welsem, T., Poramba-Liyanage, D.W., Smith, D.E., Velds, A., Hoekman, L., Korthout, T., Hendriks, S., Altelaar, A.F.M*., et al.* (2016). Direct screening for chromatin status on DNA barcodes in yeast delineates the regulome of H3K79 methylation by Dot1. Elife *5*.

62. Woolstencroft, R.N., Beilharz, T.H., Cook, M.A., Preiss, T., Durocher, D., and Tyers, M. (2006). Ccr4 contributes to tolerance of replication stress through control of CRT1 mRNA poly(A) tail length. Journal of cell science *119*, 5178-5192.

63. Yan, Z., Costanzo, M., Heisler, L.E., Paw, J., Kaper, F., Andrews, B.J., Boone, C., Giaever, G., and Nislow, C. (2008). Yeast Barcoders: a chemogenomic application of a universal donor-strain collection carrying bar-code identifiers. Nat Methods *5*, 719-725.

64. Zegerman, P., and Diffley, J.F. (2010). Checkpoint-dependent inhibition of DNA replication initiation by Sld3 and Dbf4 phosphorylation. Nature *467*, 474-478.

65. Zeman, M.K., and Cimprich, K.A. (2014). Causes and consequences of replication stress. Nat Cell Biol *16*, 2-9.

66. Zou, L., and Elledge, S.J. (2003). Sensing DNA damage through ATRIP recognition of RPA-ssDNA complexes. Science (New York, NY) *300*, 1542-1548.

SUPPLEMENTARY FIGURES AND LEGENDS

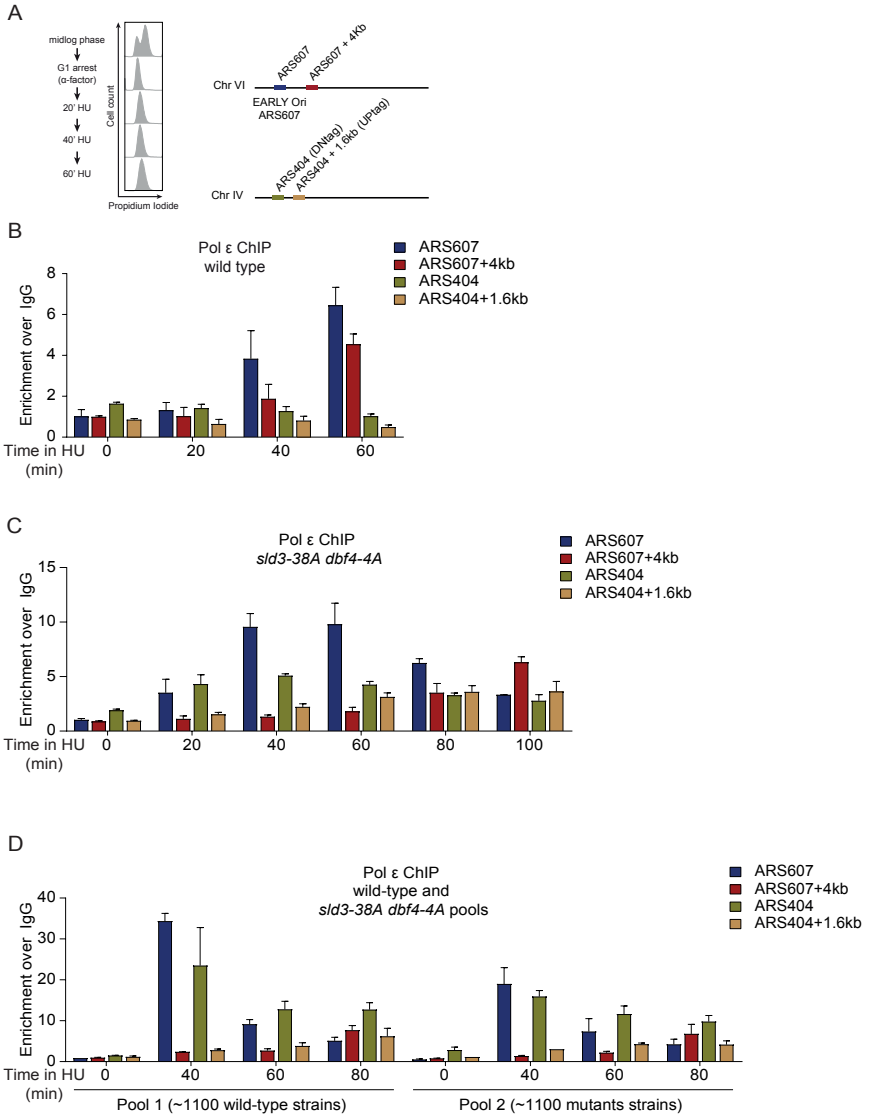

S1 Figure. Optimizing Repli-ID conditions by by ChIP-qPCR.
(A) Set-up of the ChIP experiments to study protein binding at and near ARS607 and ARS404. Left panel depicts the synchronized release of cells from G1-arrest. Right panel shows an overview of the qPCR amplicons at and near ARS607 and ARS404 studied in the ChIP experiments. ChIP-qPCR analysis of Pol e-9xMyc at ARS607 and ARS404 in (B) WT, (C) *sld4-38A dbf4-4A* strains, (D) pooled barcoded *sld4-38A dbf4-4A* mutant and WT strains. Data represent the mean relative fold enrichment of antibody signal over IgG signal in at least three independent experiments ± s.e.m. Values were normalized to unreplicated regions (ARS607+14kb).